Article

Delimiting Pig Slurry Affected Subsurface Areas by Combining Geophysical and Geochemical Techniques

Ximena Capa-Camacho [1], Pedro Martínez-Pagán [1,*], Marcos A. Martínez-Segura [1], María Gabarrón [2] and Ángel Faz [2]

1 Department of Mining and Civil Engineering, Universidad Politécnica de Cartagena, 30203 Cartagena, Spain; ximena.capa@upct.es (X.C.-C.); marcos.martinez@upct.es (M.A.M.-S.)

2 Sustainable Use, Management and Reclamation of Soil and Water Research Group, Escuela Técnica Superior de Ingeniería Agronómica, Universidad Politécnica de Cartagena, Paseo Alfonso XIII, 52, 30203 Cartagena, Spain; mariags86@gmail.com (M.G.); angel.fazcano@upct.es (Á.F.)

* Correspondence: p.martinez@upct.es

Abstract: In Spain, livestock farming is a significant activity area that generates substantial revenues and essential jobs. However, the actual impact that this intensive activity might have on the environment is not entirely understood. Moreover, coastal aquifers are subjected to a significant environmental pressure due to nearby growing population, intensive agriculture, and livestock farming. In this work, three representative pig slurry ponds, under semiarid conditions, were studied using different techniques to evaluate the subsurface conditions in terms of pH, electrical conductivity, salts, and nitrate content. The electrical resistivity tomography (ERT) technique was employed in this study, which provides electrical resistivity values from the subsurface materials and fluids. These electrical resistivity values were compared to data obtained from geochemical analyses to derive their relationships and establish the pig slurry-affected subsurface area. Thus, ERT-based lower electrical resistivity values were associated with higher salts concentrations and nitrate content. ERT values indicated a near-surface affected by slurry infiltration that coincided with the increase of geochemical values obtained from sample analyses. Additionally, Spearman's correlation was used to evaluate the correlation between electrical resistivity data and the physical-chemical properties of soil. The most important pollutant accumulation mainly occurs in the two-meter depth. Therefore, the risk of slurry ponds affecting deep aquifers is limited in the studied area. Finally, this study proves a complete, affordable, and scalable methodology application to livestock residue storage facilities.

Keywords: electrical resistivity tomography; pig slurry pond; pollutants infiltration; groundwater aquifers

1. Introduction

In 2020, Spain ranked first in Europe in livestock production, with 32.6 million head of pigs [1], which generated a volume of approximately 75 million cubic meters of slurry.

In Spain, the increase in the number of animals in the pig sector is still considerable. It has significant repercussions on the proliferation of livestock farms and, therefore, the increment in the number of slurry ponds. The region of Murcia, in terms of pig production, has a census of 2,120,000 heads [1] and a consequently associated economic and environmental impact.

Moreover, there is a coastal aquifer that has been influenced by an important increase in population, intensive agriculture, and livestock farming. Hence, these factors influence a reduction in the available groundwater and its quality, the consequences of which are not known yet.

Traditionally, the identification and characterization of potentially contaminated areas are based primarily on soil and groundwater sample analysis. This identification requires intensive borehole drilling for appropriate sampling [2]. With this drilling, we can obtain

complete information on the current situation of the sites. However, the application of non-intrusive geophysical methods allows, in a more convenient way, to develop an idea of how the contaminant plume is developed in the subsurface and how the contaminants migration mechanism works.

Geophysical methods applied to the study of contaminated areas have proven their usefulness in providing precise information on the extent of subsurface contaminants and the constitution of the most superficial subsoil [3–5].

Aracil-Ávila et al. (2003) [6] mentioned that electrical resistivity tomography (ERT) is probably the most versatile geophysical method to analyze contaminated subsoil. Thus, electrical resistivity methods should be equally valuable for characterizing and detecting leaks from livestock waste storage ponds [7].

Some authors have described relevant works applying the ERT method to monitor solute contamination plumes in a water-bearing context [8–10]. Yan et al. (2022) [11] mentioned that ERT was able to efficiently, cost-effectively, and non-intrusively detect plumes of organochlorine-based contamination in soil and groundwater within a pesticide plant in northeastern China. Furthermore, Liao et al. (2018) [12] demonstrated that ERT can characterize the extent of a plume of inorganic contaminants by comparing resistivity and soil profiles, coinciding with the variation of total iron content in the soil.

ERT method is also used to assess subsurface phosphorus and potassium content in unsaturated areas associated with high concentrations of nitrates, sulfates, and chlorites [13,14]. Guireli Netto et al. (2020) [15] demonstrated that the use of 3D ERT models allows the identification of the behavior and possible migration of a contaminant plume. In the same way, Simyrdanis et al. (2018) [16] concluded that the use of ERT can be successfully used in the monitoring of an organic waste contaminant plume, such as residues from olive oil mills.

Although research in this field is still under development to give appropriate answers to some uncertainties, we can, however, emphasize some relevant works associated with the problem above mentioned: Sainato et al. (2012) [13] and Malleville (2010) [17] concluded that electrical resistivity values are sensitive to the detection of the occurrence of animal waste leaching. These types of animal residue are characterized by higher conductive anomalies obtained in soil and groundwater sampling. In the same way, Lemeillet (2016) [18] found that electrical resistivity on a short scale displayed sensitivity to organic matter content from cattle manure.

Martínez-Pagán et al. (2009) [19] pointed out that it is necessary to have information about the physical integrity of slurry ponds to avoid potential risks of environmental pollution. A defective slurry pond can increase eutrophication problems of surface and groundwater with high amounts of PO_4^{3-}, NO_3^-, and NH_4^+ and salinization, phytotoxicity, and nutritional imbalances filtration into aquifers as well as damage to soils.

In this way, the slurry infiltration generated in the subsoil can be derived from a specific correlation between variations in soil, slurry chemical properties, and electrical resistivity values collected by the electrical resistivity tomography technique.

Therefore, the main objective of this work is to provide a validated methodology that combines the use of the electrical resistivity tomography (ERT) method, boreholes with core sampling, and geochemical soil analysis. This combination of different methods will permit obtaining information on the impact and infiltration of slurry under slurry ponds.

1.1. Study Site

Fuente Álamo is one of the municipalities forming part of the region of Murcia (Figure 1). This area is characterized by a Mediterranean semiarid climate, with an average temperature of 18 °C and annual average precipitation of 300 mm [20].
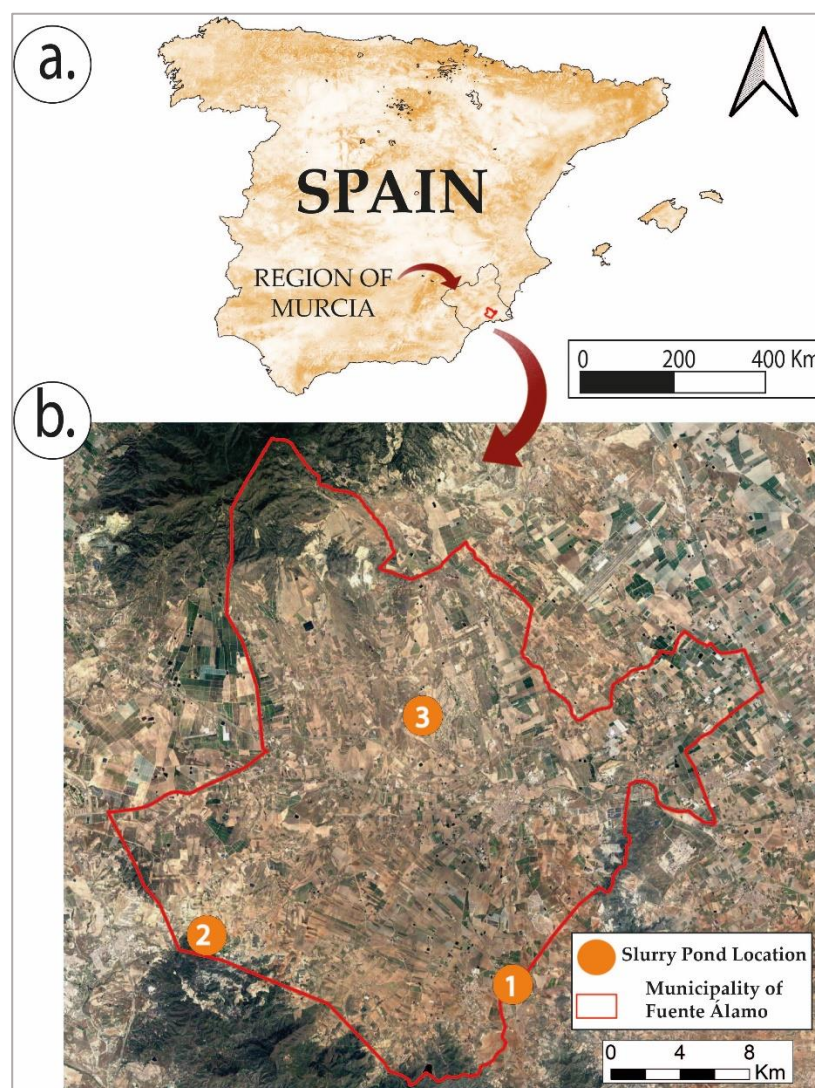
Figure 1. Geographical location of (**a**) the municipality of Fuente Álamo, and (**b**) the three studied slurry ponds.

The geology of the area is part of the "Campo de Cartagena", formed by a thick Neogene-Quaternary basin, which corresponds to the Internal Betics domain. The lithology comprises Quaternary deposits, constituted by "caliche" petrocalcic horizon, conglomerates, alluvial clays, silts, and sands [21].

The hydrogeology of this area is characterized by the presence of three main aquifers: (a) Quaternary "Campo de Cartagena" aquifer, (b) Triassic "Las Victorias" aquifer, and (b) Triassic "Carrascoy" aquifer. The Campo de Cartagena aquifer thickness ranges from 50 to 150 m of gravels, sands, silts, clays, and caliche deposits in which the aquifer depth is about 30 m at the study area, becoming shallower to the coastline. The "Las Victorias" aquifer thickness is roughly 50 m of Triassic marble underlying Permo-Triassic schists, cuarcites, and gneisses from the deposits and terraces Nevado-Filabride in which the aquifer is found at 500 m depth. Finally, the "Carrascoy" aquifer thickness ranges from 200 to 250 m of Triassic dolomites in which the aquifer depth is determined at 300 m [22,23].

On the other hand, the approximate total number of farms in the municipality of Fuente Álamo is around 265 pig farms.

At this point, this research has focused on three representative slurry ponds situated in geologically different areas in the municipality of Fuente Álamo in order to determine at each selected slurry pond: (a) differential slurry infiltration behavior, (b) associated electri-

cal resistivity characteristics, and (c) concentration changes, especially the concentrations that may indicate a possible slurry infiltration (pH; EC; salts, such as Cl^- SO_4^{2-}, and Na^+; and the amount of nitrates $N-NO^{3-}$).

The investigation was carried out in each slurry pond by means of ERT studies, mechanical drilling with the extraction of soil samples, and geochemical analysis. It is worth recalling that mechanical drilling was conducted outside the pig slurry pond to avoid any potential subsurface contamination during the drilling operation. The depth of drilling ranged from 10 to 15 m and provided undisturbed samples for chemical analyses by means of diamond coring systems.

1.2. Pig Slurry Ponds

A pig slurry is a liquid mixture of excrement, urine, food scraps, cleaning water, and other residues. The composition of this mixture is variable and dependable on many factors related to the livestock activities undertaken [24].

Temporary storage facilities, called slurry ponds, have been built on each livestock farm because of the considerable amount of slurry generated, which must be appropriately stored during livestock activities.

These slurry ponds are built under various sizes and geometries; however, the most usual geometry is the rectangular one. In this case, a rectangular outer earthen rim would be mechanically made, which acts as a barrier against any slurry overflow. The material employed to make the outer earthen rim is the soil extracted from the bottom of the slurry pond.

The depth of the slurry pond ranges from a few centimeters to three meters. The deepest slurry ponds keep the pig slurry stored for longer periods or even all year long, based on its use as liquid-based agriculture fertilizer. Hence, their slurry-storage activity is considered continuous. Conversely, the shallower ones encourage the slurry to dry for manure production and its use as a solid-based agriculture fertilizer. As a result, this slurry-storage activity is considered periodical. It is noteworthy that the slurry ponds selected in this study were constructed without any artificial waterproofing, such as a rubber liner or a layer of concrete. Therefore, the impermeability of the pond against slurry infiltration will rely mainly on the lithological characteristics of the site.

The measurements were carried out in September 2020 in the three slurry ponds located in the municipality of Fuente Álamo. At that time the slurry pond No. 1 was found almost dried with only some patches of slurry and the remainder being manure. Slurry pond No. 2 was found completely full of slurry in which the percentage of water content was high. This slurry pond is considered a deep slurry pond. Finally, the slurry pond No. 3 was found full of slurry as well. This slurry pond is considered a shallow slurry pond.

2. Materials and Methods

Three slurry ponds located in the municipality of Fuente-Álamo were chosen. This choice was done according to the type of soil found in this municipality. Thus, each slurry pond was in a different type of soil (Figure 2). At each slurry pond, the geophysical methodology consisted of implementing parallel external and internal profiles of ERT (Figure 3). Moreover, a borehole was conducted at each slurry pond to collect core samples for geochemical analyses.

In addition, the ERT layout was established according to the slurry pond size (Figure 3). This layout was defined as follows:

- Five profiles were carried out at slurry pond No. 1. Three of them were external profiles (named Ep1, Ep4, and Ep5, respectively), with one meter between profiles. The other two were internal profiles (labeled Ip2 and Ip3, respectively), with a separation of seven meters between them (Figure 3a).
- Three external profiles were carried out at slurry pond No. 2. Here, external profile No. 1 (Ep1) was placed externally on one side, and the other two external profiles

(Ep4 and Ep5) were on the other side (Figure 3b). Additionally, two internal profiles (named Ip2, and Ip3, respectively) were laid out six meters apart (Figure 3b).

- Seven profiles were carried out at slurry pond No. 3 (Figure 3c). Four of these profiles (Ep1, Ep2, Ep6, and Ep7) were external profiles, where two of them were laid out on one side and the other two on the other side (Figure 3c). Internal ERT profiles (Ip3, Ip4, and Ip5) were laid out with a profile spacing of five meters (Figure 3c).

The main objective of employing external ERT profiles was to electrically image the influence of any lateral infiltration that occurred from the slurry pond. On the other hand, internal ERT profiles had the main objective of electrically imaging the vertical slurry infiltration underneath the slurry pond.
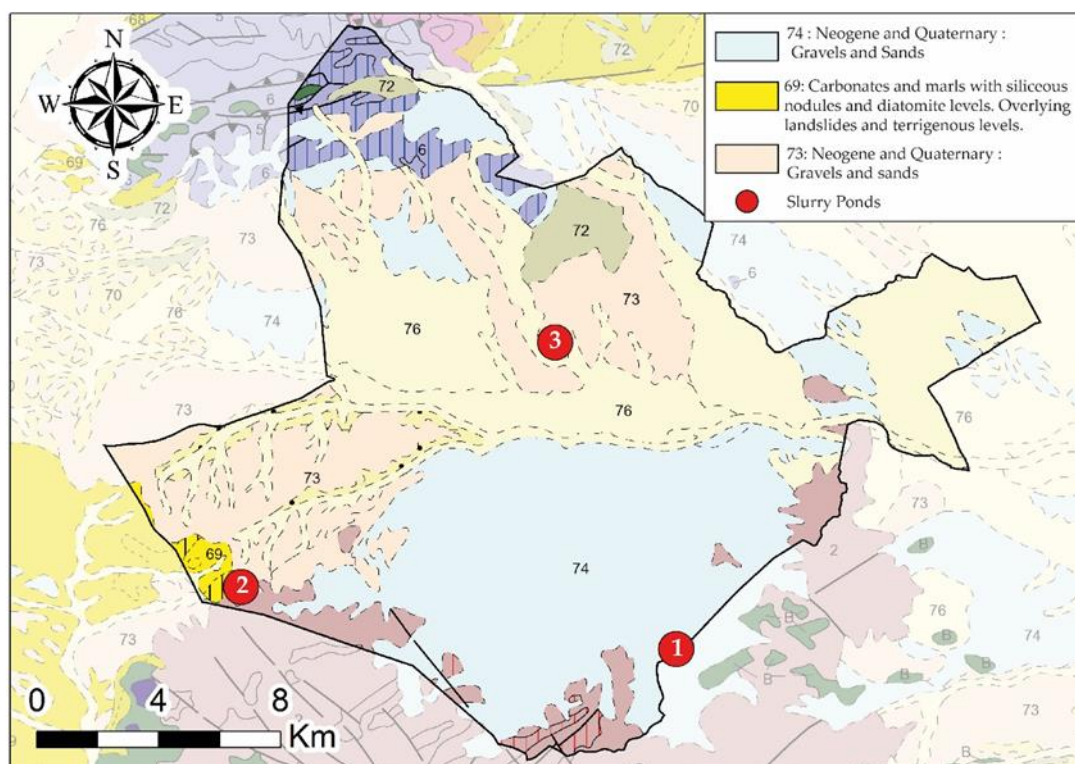

Figure 2. Geological map of the Region of Murcia (1:200,000) (Source: GEODE, Spanish Geological Survey (IGME)).

2.1. Electrical Resistivity Tomography (ERT) Method

The ERT method is an applied and non-invasive geophysical technique to detect complex geological structures in the subsurface [25].

This electrical-based technique relies on the contrast of electrical resistivity values associated with subsurface material and fluid content [26]. Electrical resistivity values are highly influenced by soil conditions, e.g., particle size distribution, mineralogy, porosity, pore size distribution, water content, solute concentration, and temperature [8].

ERT method consists of implementing a series of grounded electrodes. With respect to ERT profiles, the number of electrodes employed was 28 [25]. Electrode inter-spacing will influence the resolution of the investigation, which refers to the smallest subsurface object that can be detected by the ERT method. Thus, the smaller the separation between electrodes, the higher the obtained resolution [6].

SLURRY POND No.1

SLURRY POND No.2
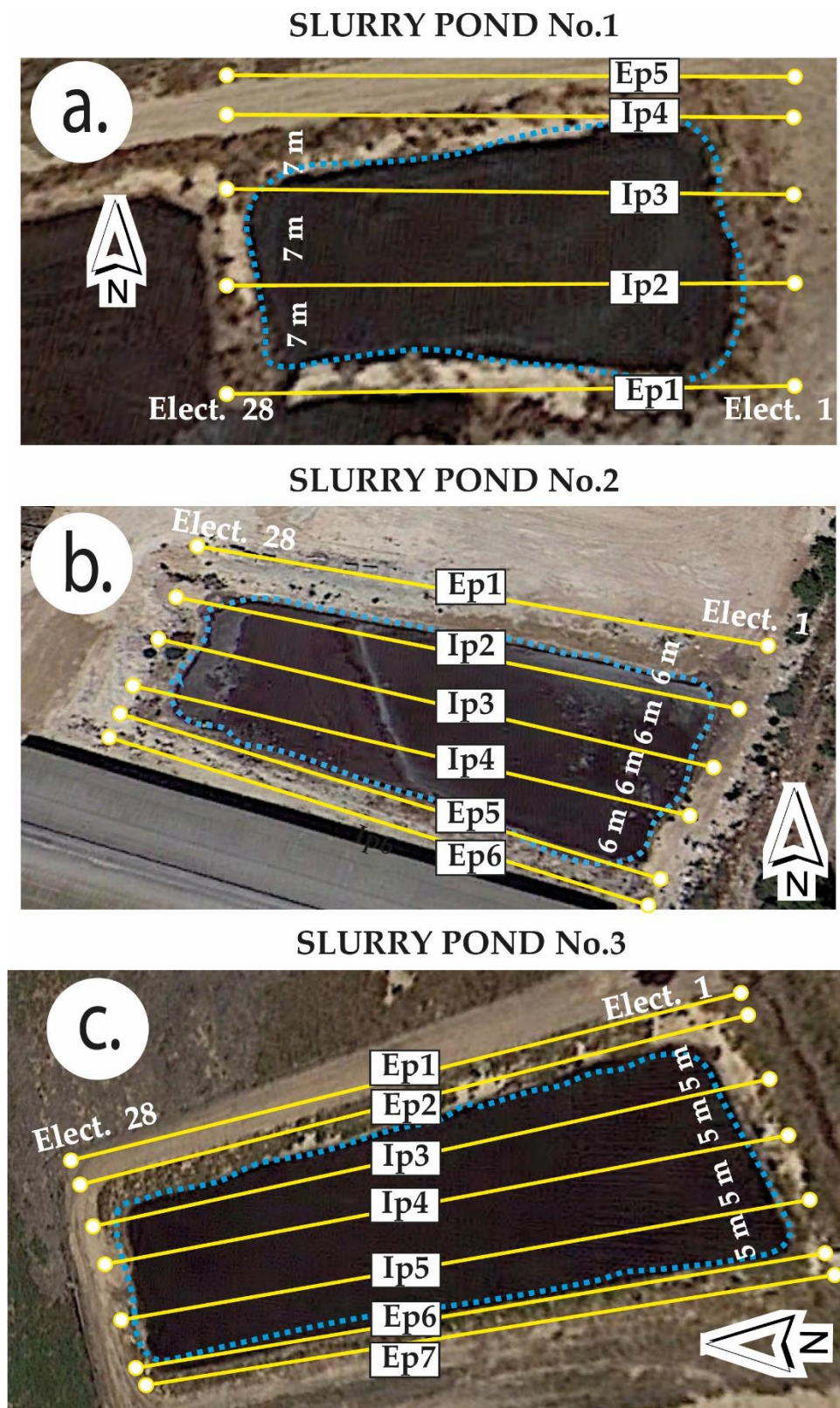
SLURRY POND No.3

Figure 3. Schematic layout of ERT external and internal profiles at (**a**) slurry pond No. 1, (**b**) slurry pond No. 2, and (**c**) slurry pond No. 3.

In this work, the electrode spacing was one meter in slurry pond No. 1 and two meters in slurry ponds No. 2 and No. 3. That chosen electrode spacing was largely determined

by the slurry pond geometry. The electrical system constituted a switch box to which the electrodes were connected by means of an isolated multicore cable [27].

As the primary electrical recording unit, a SuperSting R8 resistivity meter from Advanced Geosciences Inc. was used to obtain the subsurface apparent electrical resistivity values at each slurry pond (Figure 4a).

Regarding internal ERT profiles, these were laid out employing a waterproof marine cable equipped with graphite electrodes since slurry ponds were found full of slurry (Figure 4b). These graphite-made electrodes were kept on the slurry surface with the help of polyethylene floats, which were attached to the marine cable using plastic clamps (Figure 4b).
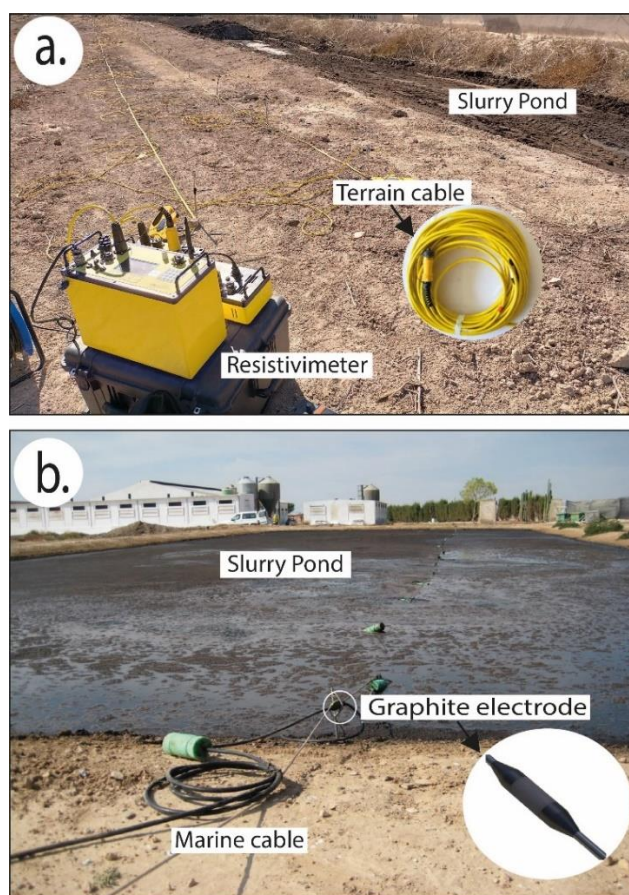
Figure 4. Typical set up of (**a**) an ERT external profile and (**b**) an ERT marine profile.

For the subsurface electrical resistivity measurements, a dipole–dipole array was used. This type of measurement configuration has proved an appropriate depth of penetration [26,28]. Furthermore, this array is particularly sensitive to lateral variation with depth, which makes it more favorable for detecting lateral variations in non-homogeneous zones [29].

Once the apparent resistivity values were obtained from field measurement campaigns, they were processed through the AGI EarthImager 2D/3D software package. This data postprocess mainly consisted of isolating and removing anomalous data and inversion processing steps. Inverse simulation allowed obtaining the actual subsurface resistivity properties under 2D electrical sections and 3D electrical blocks. With regard to inverse modeling, this was based on smooth model inversion, also known as Occam's inversion, whose response fits the data to an a priori chi-square statistic. In line with that, the true model must be at least as the smooth model obtained through smooth model inversion. The smooth model inversion algorithm was originally described in Constable et al. (1987) [30]

and DeGroot-Hedlin and Constable (1990) [31]. These models were obtained with a minimum of eight iterations and a root mean square (RMS) error below 10%, which means a reduced data misfit between field measurements and calculated data of the models. Another data misfit that could be used is L2 norm (L2), defined as the sum of the squared weighted data errors in which values near to the unity or smaller means that the inversion is converged [32]. Three-dimensional electrical blocks were obtained by inversion as pseudo-3D survey with the combination of the parallel 2D ERT profiles using EarthImager3D software [32], which produces a 3D volume image and gives a better resolution of the subsurface. A 3D data set formed this way is considered a pseudo-3D data set because cross-line measurements with transmitting and receiving electrodes on different lines are not taken [33]. Since the reality is not 2D but 3D, it is recommended to compare or assess 2D and 3D results [33].

These 2D electrical sections and 3D electrical blocks enabled us to assess and infer the subsurface pig slurry affected region and if that could mean any risk to the most surficial aquifers of the study area.

2.2. Characterization of Soil Properties

The geophysics stage was followed by the drilling stage (Figure 5a). This stage consisted of borehole drilling at each slurry pond and the gathering of column core samples (Figure 5b).
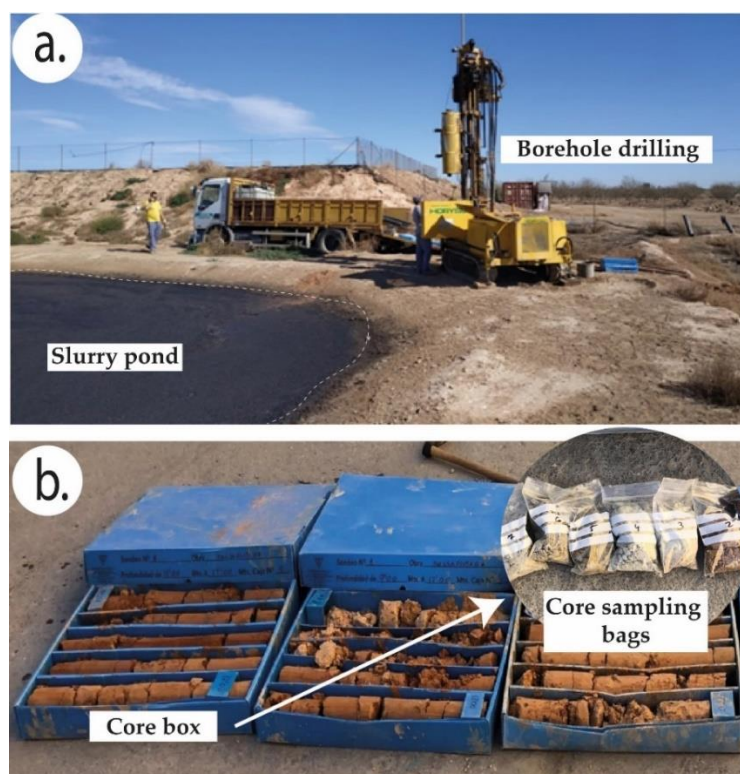
Figure 5. (**a**) Drilling operation at the slurry pond; (**b**) core samples collected from a borehole.

The previous ERT survey determined the borehole position. Thus, the drilling rig was situated in those more conductive areas near the slurry pond characterized by lower electrical resistivity values since it is considered that lower electrical resistivity values are likely associated with the presence of slurry in the subsoil.

The depth reached by the boreholes was approximately 15 m. Core samples were simultaneously taken during borehole drilling operations and appropriately placed in sample boxes (Figure 5b). The adopted criterion was to take samples from every meter

depth or at each detected change in the lithology column. On average, 15 core samples were obtained from each borehole. Then, these core samples were subjected to laboratory analyses to obtain the most representative physicochemical parameters of soils (Figure 5b).

Geochemical characterization of each lithology was considered during the soil analysis stage. The analyses carried out on the soil samples were the determination of pH [34], electrical conductivity [35], soluble salts, total nitrogen content, and particle size distribution.

The pH and electrical conductivity (EC) were measured in a soil sample, with a deionized water ratio of 1:2.5 *w/v* (weight/volume) and 1:5 *w/v*, respectively. The pH and CE tests were conducted using selective electrodes [34,35]. Soluble salts were obtained from an extract of fresh soil in proportion 1:5 *w/v* and quantified by ion chromatography using a Methrom 850 Professional by IC. Additionally, the total nitrogen (TN) content was measured using a CHN 628 elemental analyzer by Leco. Finally, the particle size distribution was obtained using a Mastersizer 2000lf laser diffractometer by Malvern Instruments.

2.3. Statistical Analysis

In order to assess the correlation between the electrical resistivity data and the chemical properties of soil, a bivariate correlation test should be carried out. To ensure the fitting of the data into a normal distribution, the Kolmogorov–Smirnov normality test at $p < 0.05$ was used. Thus, the K-S results showed that data non-fitted normality. Therefore, the selected test to study the statistical correlation was the Spearman correlation non-parametric test. The software SPSS Statistics v.23 (IBM, New York, NY, USA) was employed to accomplish that assessment.

3. Results and Discussion

3.1. Borehole Samples and Physicochemical Analyses

Figure 6 shows the lithological columns obtained from drilling operations in the three slurry ponds corresponding to Quaternary deposits [21]. These lithological results (from BH1, BH2, and BH3 borehole) are in line with those presented by Martínez-Pagán et al. (2010) [36], who identified the presence of caliche horizons alternating with layers of gravel and clay. BH1 borehole, which corresponds to slurry pond No. 1, shows a layer of silts and clays with intercalations of sands up to 1.8 m in depth. Then, a layer of carbonate crust follows with a thickness of 2.4 m; and underlying, there is a layer of purplish shales that are highly weathered with a thickness of 10.8 m (Figure 6a). BH2 borehole, which corresponds to slurry pond No. 2, presents a layer of silts and clays with sand intercalations with a thickness of 2.5 m, followed by a layer of sandstones with a thickness of 12.5 m. Similarly, for slurry pond No. 3, the BH3 borehole defines the presence of a single layer corresponding to silts and clays with sandstone intercalations.

At this point, geochemical analyses carried out on samples collected from boreholes showed relevant physicochemical variations. Thus, Table 1 shows these physicochemical variations based on the following parameters: pH, EC, salts (Cl^-, SO_4^{2-}, Na^+), and nitrates (N^- and NO_3^-) content. At Fuente Álamo area, the pH of soils presents values between 8.2 and 9.42, which corresponds to alkaline soils [26]. In the three surveys carried out, a variation of the pH value is observed for the first meters of depth (Table 1). These values tend to stabilize at more depth. From BH1 borehole samples, pH values range between 8.2 and 8.49 along the first 1.80 m of depth. On the other hand, from BH2 borehole samples, up to 2.2 m, pH values range between 8.24 and 8.16. Finally, from BH3 borehole samples, pH values vary between 8.31 and 8.89 up to 2.10 m. Straczynska (1994) [37] and Chang et al. (1990) [38] associated the decrease in soil pH with subsurface pig slurry accumulation since high salt content caused soil acidification.
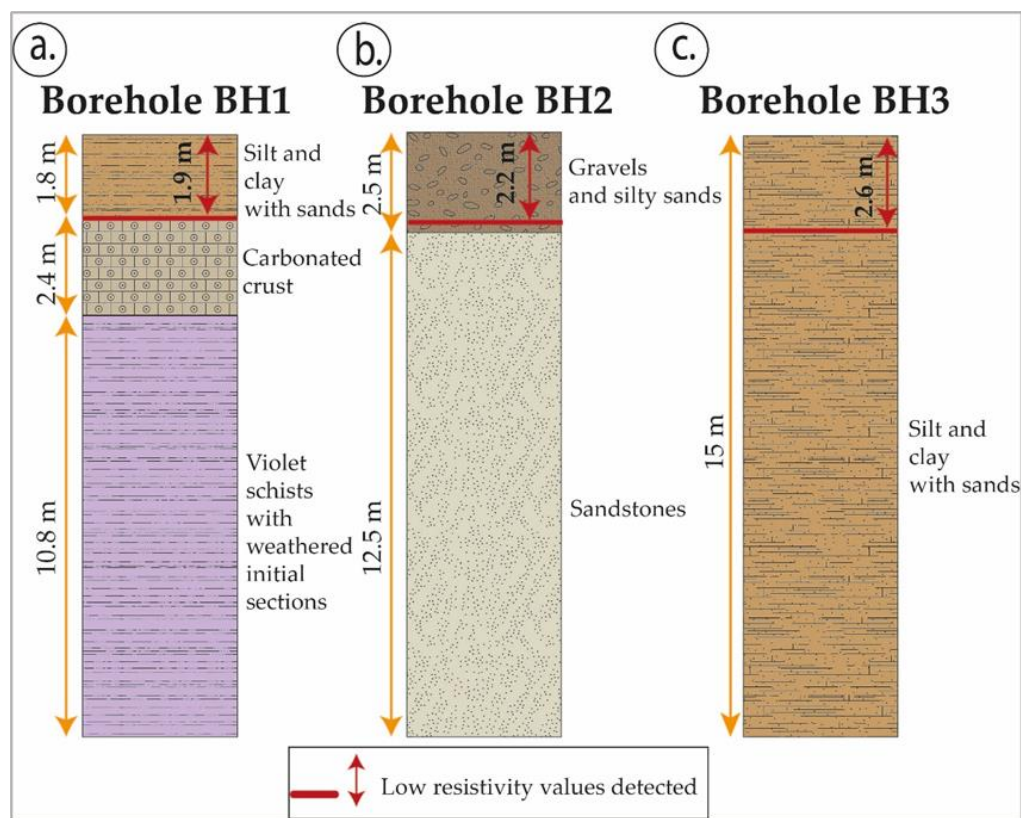
Figure 6. Lithology columns from drilling operations in (**a**) slurry pond No. 1, (**b**) slurry pond No. 2, and (**c**) slurry pond No. 3.

Table 1. Main values from geochemical analysis on soil samples. The increase observed in the two-meter depth in the main parameters is framed.

Depth (m)	Moisture (%)	pH	EC (dS/m)	Cl^- (mg/kg)	SO_4^{2-} (mg/kg)	Na^+ (mg/kg)	Mg_2^+ (mg/kg)	$N\text{-}NO_3^-$ (mg/kg)	Clay %	Silt %	Sand %
Slurry Pond No. 1											
−1.00	10.66	8.20	0.80	657.26	58.63	160.97	49.07	97.60	9	37	55
−1.80	15.97	8.49	0.37	234.12	58.74	66.76	51.26	45.05	20	68	13
−3.00	7.47	9.03	0.16	24.98	37.63	19.99	13.07	2.80	10	65	26
Slurry Pond No. 2											
−1.00	17.72	8.24	3.75	5644.25	2897.67	2544.33	1337.70	951.90	3	49	49
−2.20	16.32	8.16	2.72	1559.65	1233.43	812.85	137.84	746.83	6	42	52
−3.00	14.53	8.54	1.42	1154.21	1059.64	553.02	74.37	423.32	3	42	55
Slurry Pond No. 3											
−1.50	6.02	8.31	0.81	267.03	885.18	257.40	82.70	143.29	12	47	41
−2.10	10.13	8.89	0.13	77.70	112.77	73.49	25.36	9.38	9	54	37
−4.20	6.21	8.77	0.16	0.00	191.03	53.63	23.68	1.93	9	53	39

EC values, assigned to non-contaminated soils of the municipality of Fuente Alamo, range between 0.1 and 0.2 dS/m. It is worth noting that EC and pH are somehow interrelated since any increase in soil salt concentration (e.g., nitrate content) will influence pH and EC increase and decrease in pH [39] Therefore, slurry infiltration, in contact with the soil, increases the content of salts and other ions that are likely to lixiviate [8,13,17,40] Thus, Table 1 shows a significant increase in EC, Cl^-, SO_4^{2-}, and Na^+ content for those surficial horizons near slurry ponds.

BH1 borehole samples provide EC values ranging from 0.80 to 0.37 dS/m into a depth of 1.80m. Those EC values establish that the highest EC value is in the first depth meter. Similarly, an increase in Cl^-, SO_4^{2-}, and Na^+ concentration is observed near-surface. At this point, the highest concentrations correspond to Cl^- ion, with a 657.26 mg/kg concentration, and Na^+ ion, with 160.97 mg/kg.

BH2 samples show much higher values of EC (between 3.75 and 2.72 dS/m up to a depth of 2.20 m). Additionally, the highest ion concentration is obtained for the first meter. Similarly, to BH1 samples, the ion concentration is higher for Cl^- ion, with 5644.25 mg/kg for the first meter. Therefore, the increase in the concentration of salts (Cl^-, SO_4^{2-}, and Na^+) and EC values can be attributed to near-surface slurry infiltration. In fact, Carrasco (2005) [41] demonstrated how applying slurry in the soil promotes EC value increases. Carnol et al. (1997) [42] attributed the increase in soil SO_4^{2-} concentrations to slurry-amended crop soils, similarly to the accumulation of Cl^- at the surface [43].

In addition, BH3 samples present EC values between 0.81 and 0.13 dS/m to a depth of 2.10 m, in which the highest EC value is located near-surface at 1.50 m depth. In line with that, salts content, attributed to Cl^-, SO_4^{2-}, and Na^+ ion presence, also shows an increase. The highest concentration is associated with SO_4^{2-}, with 885.18 mg/kg up to 1.50 m depth.

BH1 and BH3 sample data show similar increases in EC value. This increase may be associated with lithology-related characteristics since conductive properties are associated with silts and clays horizons [44], whose presence has been determined by boreholes.

For this type of lithology, the pig slurry infiltration rate shows a decrease [45], which is attributed to the presence of clay and silt horizons. Clay and silt particles have the property of reducing pig slurry flow throw subsurface voids [45–47].

Thus, BH1 and BH3 samples values contrast to those observed from BH2 samples, which are mainly composed of gravel with silty sands to a depth of 2.5 m. In this case, the present texture allows a higher porosity and therefore a higher infiltration rate of pig slurry to the subsurface [45].

On the other hand, nitrogen content values have been derived knowing that nitrogen content in the soil is mainly due to biological processes and crop fertilizing [48]. Many authors attribute the surface concentrations of nitrate in the soil directly to the effect of pig slurry [17,49]. Daudén and Quílez (2004) [50] indicated that pig slurry-based fertilization of crops increased soil nitrate concentration in a Mediterranean environment and under irrigated conditions. Thus, nitrate content (e.g., $N-NO_3^-$) is an excellent indicator of nitrogen lixiviation into the subsurface [51]. Nitrate values derived from borehole samples show a notable increase in $N-NO_3^-$ content for the same depth in which high values of pH, EC, Cl^-, SO_4^{2-}, and Na^+ are obtained. In this way, the highest $N-NO_3^-$ concentration value corresponds to 97.60 mg/kg, 951.90 mg/kg, and 143.29 mg/kg for BH1, BH2, and BH3, respectively.

3.2. Electrical Resistivity Tomography Models and Statistical Correlations

The 2D ERT electrical sections and 3D ERT electrical blocks show different resistive zones in each slurry pond. The 2D electrical sections with the highest resistivity values correspond to the external ERT profiles.

These electrical resistivity values range between 21.8 and 104 Ohm.m, which agree with the values obtained by Martínez-Pagán et al. (2009) [19] for the Fuente Álamo area. These high resistivity values contrast with the values obtained from internal ERT profiles, ranging from 0.2 to 4.6 Ohm.m.

As aforementioned, geochemical soil analyses showed variations with depth in the concentrations of pH, EC, salts (e.g., Cl^-, SO_4^{2-}, Na^+), and nitrates (e.g., $N-NO_3^-$). The depth at which these noticeable variations occur coincides with electrical changes derived from 2D/3D ERT surveys.

Thus, for slurry pond No. 1 (SP1), ERT surveys provide the lowest electrical resistivity values ranging from 1 to 5 Ohm.m to a depth of 1.9 m (Figure 7). Therefore, these results align with those high values obtained from the geochemical analysis, which shows variations up to a depth of 1.8 m (Table 1). With regard to the conductive areas in Figure 7 delimited with Ip3 and Ip2 ERT profiles, these are patches of slurry, with the remainder region being almost solid manure in which most of the water content has been removed primarily by solar dehydration.

Slurry pond No. 2 (SP2) presents variations in the geochemical analysis up to a depth of 2.20 m (Table 1). Similarly, the lowest value of resistivity, obtained by ERT, ranges from 1 to 3 Ohm.m to a depth of approx. 3 m (Figure 8). It is worth recalling that this pig slurry pond is exceptionally full of pig slurry, with a high percentage of water content all year long and where its bottom reaches three meters depth. This relevant point could explain the relatively conductive region that shows Ip4 beneath positions from 0 to 18, which could be due to some pig slurry infiltration phenomenon occurring in that area to a depth of roughly 10 m. In fact, the near-DH2 borehole samples indicated higher geochemical values to a deeper depth compared to the other slurry ponds samples (Table 1).

Regarding slurry pond No. 3 (SP3), geochemical analyses show content variations up to a depth of 2.10 m (Table 1). In line with that, low electrical resistivity values range from 2 and 6 Ohm.m up to 2.6 m in depth (Figure 9).
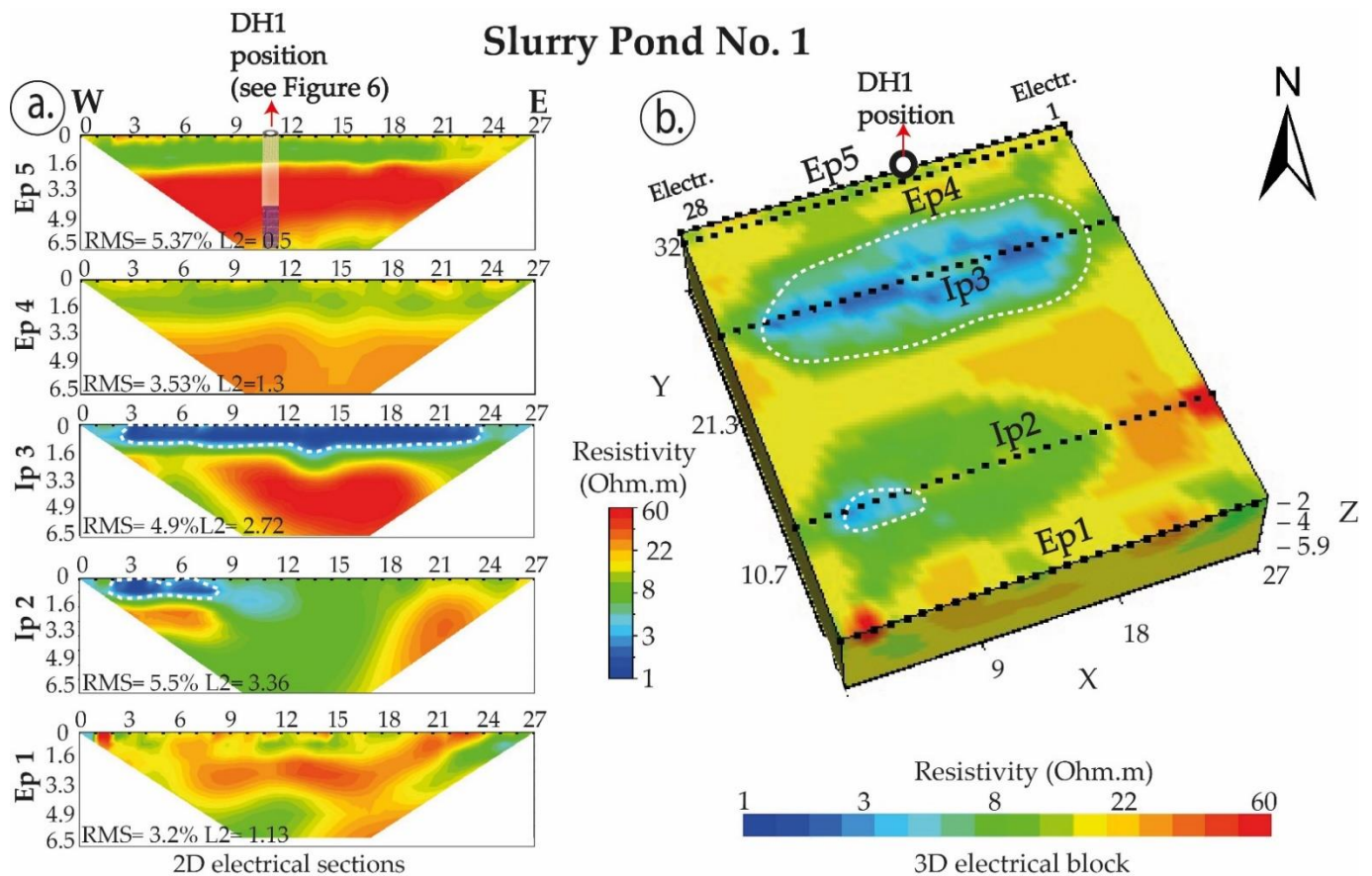
Figure 7. Slurry pond No. 1. (**a**) ERT 2D electrical sections and (**b**) ERT 3D electrical block. RMS and L2 stand for root-mean squared error and L2 norm, respectively. Electrode spacing is 1 m.
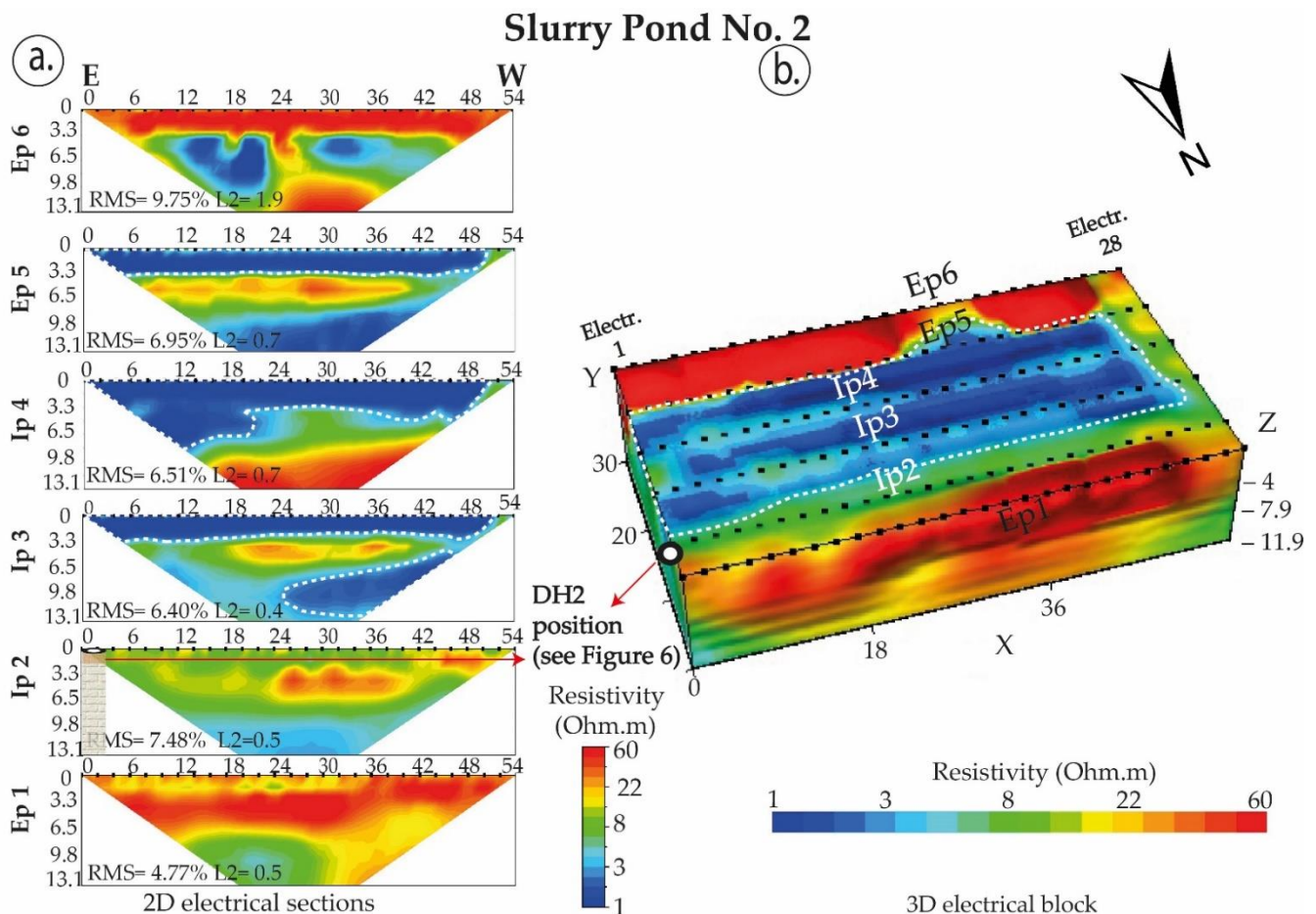
Figure 8. Slurry pond No. 2. (**a**) ERT 2D electrical sections and (**b**) ERT 3D electrical block. RMS and L2 stand for root-mean squared error and L2 norm, respectively. Electrode spacing is 2 m.

According to Peralta et al. (2015) [40], these changes in EC, nitrates, and electrical resistivity values highlight a robust spatial correlation and might indicate the possible infiltration of pig slurry. Moreover, Hernandez Ramos (2019) [52] attributed electrical resistivity values lower than 10 Ohm.m to soil slurry infiltration phenomena.

In SP1, the 2D electrical sections obtained from external ERT profiles show electrical resistivity values ranging from 9 and 84 Ohm.m (Figure 7).

Statistical analysis does not show significant correlation between moisture content and resistivity values for external profiles; however, it shows, for external profile No. 1 (Ep1), a significant correlation among resistivity values and silt percentage (R = 0.639; $p < 0.05$), pH (R = 0.611; $p < 0.05$), EC (R = 0.667; $p < 0.05$), and N-NO_3^- (R = 0.611; $p < 0.05$).

These results suggest that resistivity values from external profiles could correlate directly to soil texture, pH, EC, and nitrate (N-NO_3^-) content. The noticeable correlation between ERT-based resistivity and analysis-based EC values is strongly influenced by particle size conditions, which are directly related to the electrical charge density that occurs on the particle surface [19].

The internal profiles No. 2 (Ip2), and No. 3 (Ip3) show positive bivariate correlation with pH values and resistivity (R = −0.919; $p < 0.01$); (R = −0.802; $p < 0.01$) and negative bivariate correlation between resistivity and EC (R = −0.881; $p < 0.01$); (R = −0.849; $p < 0.01$). This positive correlation suggests that pH values directly correlate with resistivity values; i.e., as pH alkalinity of soil decreases, resistivity values are expected to decrease as well. This correlation is observed in the soil analyses (Table 1), where resistivity values tend to decrease.
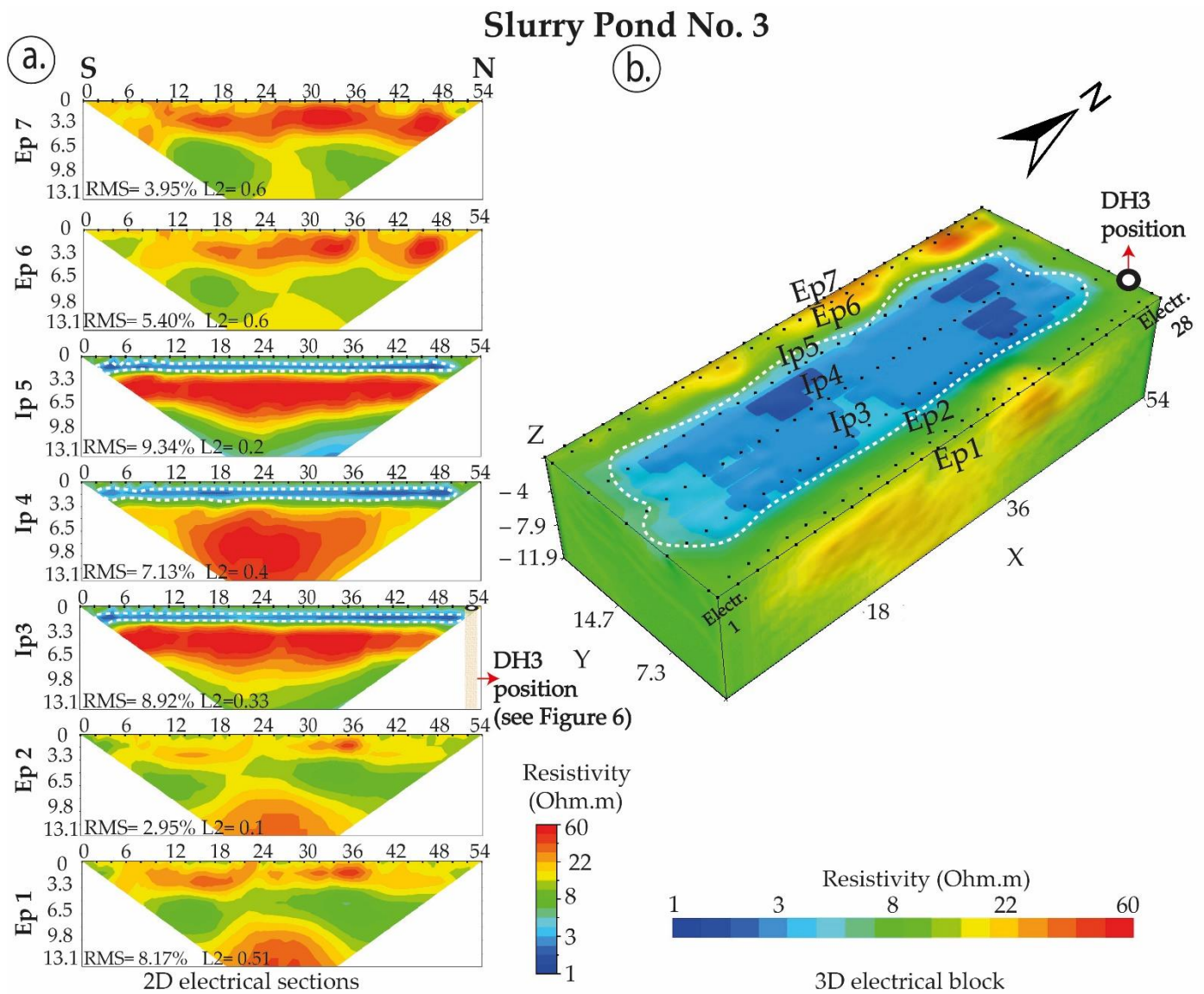
Figure 9. Slurry pond No. 3. (**a**) ERT 2D electrical sections and (**b**) ERT 3D electrical block. RMS and L2 stand for root-mean squared error and L2 norm, respectively. Electrode spacing is 2 m.

The negative bivariate correlation between resistivity and EC suggests that with the possible infiltration of slurry, and as a result, an increase in the content of salts, organic matter, P, N, and other inorganic and organic ions [37,47] causes the electrical resistivity values to tend to decrease.

In the same way, a significant negative correlation is observed for Cl^- ion (R = −0.870; $p < 0.01$), (R = −0.790; $p < 0.01$); SO_4^{2-} ion (R = −0.835; $p < 0.01$), (R = −0.737; $p < 0.01$); and Na^+ ion (R = −0.667; $p < 0.05$), (R = −0.877; $p < 0.01$). Furthermore, N-NO_3^- shows a significant increase at this depth and presents a significant negative correlation with resistivity data in the internal profiles (R = −0.919; $p < 0.01$), (R = −0.793; $p < 0.01$).

Piñeiro and Montalvo (2015) [51] suggested that nitrate (N-NO_3^-) content may indicate nitrogen leaching. The negative correlation would support that the higher the N-NO_3^- content in the soil, the lower the expected electrical resistivity values.

The same behavior is observed in SP2. Thus, the external ERT profiles show high resistivity values, ranging from 7 to 202 Ohm.m. However, statistical analyses do not show any significant correlation between resistivity and physicochemical properties.

Conversely, internal profiles (Ip3 and Ip4) provide a decrease in resistivity values ranging from 0.8 to 20 Ohm.m to a depth of 3 m, with the exception of profile Ip4, which shows a deeper conductive area on its left-hand side. This depth range coincides with the same range at which an increase in moisture content, pH, EC, salts, and nitrate content was obtained (Table 1).

Statistical analysis showed significant negative correlations with moisture content (R = -0.697; $p < 0.05$), (R = -0.706; $p < 0.05$). The literature indicates that when the soil water content increases from dry to water-saturated soil conditions, ions previously adsorbed are released from the soil particle surface. These released ions promote the decrease of electrical resistivity that is obtained from ERT surveys [8,39,53–55]

pH values show a significant positive correlation (R = 0.754; $p < 0.01$), (R = 0.777; $p < 0.01$), as is observed in the SP1, where the values slightly decrease with the alkalinity value.

Similarly, EC, salts (Cl^-, SO_4^{2-}, and Na^+), and nitrate ($N\text{-}NO_3^-$) content show high values, which might explain lower resistivity values obtained at the same depth (Table 1).

Statistical analysis shows significant negative correlations for EC (R = -0.697; $p < 0.05$), (R = -0.706; $p < 0.05$) as well as for $N\text{-}NO_3^-$ (R = -0.789; $p < 0.01$), (R = -0.872; $p < 0.01$).

Salts (Cl^-, SO_4^{2-}, and Na^+) content, as in SP1, presents negative correlations with electrical resistivity values (R = -0.780; $p < 0.1$), (R = -0.890; $p < 0.01$) for Cl^-; (R = -0.679; $p < 0.5$), (R = -0.844; $p < 0.01$) for SO_4^{2-}; and (R = -0.761; $p < 0.1$), (R = -0.899; $p < 0.01$) for Na^+.

At SP3, external ERT sections display resistivity values ranging from 9 to 40 Ohm.m. Conversely, internal ERT sections display lower resistivity values, ranging from 2 to 6 Ohm.m, for the first 2.6 m depth.

The statistical analysis exhibits significant correlations in external profiles ep6 and ep7. Data analysis shows that electrical resistivity depicts a negative correlation with physical properties associated with moisture content (R = -0.779; $p < 0.01$), (R = -0.642; $p < 0.01$) and silt percentage (R = -0.730; $p < 0.05$), (R = -0.716; $p < 0.05$) and positive correlations with sand percentage (R = 0.693; $p < 0.05$), (R = 0.679; $p < 0.05$).

Lower electrical resistivity values are obtained from ERT internal profiles, with resistivity values ranging from 2 to 6 Ohm.m to a depth of 2.6 m. Additionally, soil analyses provide the highest content variations to a depth of 1.50 m.

The statistical analysis only reveals significant correlations with internal profile 4 (Ip4). The pH displays significant positive correlations (R = 0.789; $p < 0.01$), and conversely, nitrate shows significant negative correlations (R = -0.688; $p < 0.05$).

SP3 shows a behavior similar to that determined for the slurry ponds mentioned above (SP1 and SP2).

Data analysis reveals that lower electrical resistivity values significantly correlate with the variations obtained in the geochemical analysis of the soil samples.

The depth at which geochemical analyses underline relevant parameter variations coincides with the same depth highlighted by employing 2D ERT sections and the 3D ERT blocks.

4. Conclusions

Intensive livestock farming can result in significant environmental impacts such as direct contamination of soil and aquifers systems adjacent to final pig slurry storage facilities. The electrical properties contrast between the natural geological environment and the near-surface slurry infiltration makes the electrical resistivity tomography method highly recommended in studies of environmental impacts in livestock slurry storage facilities.

The present work demonstrates how geophysical data can delimit the subsoil affected by slurry infiltration in conjunction with geochemical ones. Under semiarid conditions and low-depth pig slurry ponds with intermittent activity, the ERT technique has established this effect of slurry at two meters depth, from which subsurface slurry content remarkably

decreases. Conversely, for deeper-depth pig slurry ponds with permanent pig slurry storage, the ERT technique shows deeper subsurface pig slurry effects from 3 to 10 m.

Further, results obtained by the electrical resistivity tomography technique agree with the values derived from soil geochemical analysis. Subsurface geochemical variations of pH, EC, salts (Cl^-, SO_4^{2-}, Na^+), and nitrates ($N-NO_3^-$) content have been established from borehole sample analyses. Moreover, subsurface horizons at which noticeable geochemical variations have been defined coincide with electrical properties characterized by conductive values.

Similar to the ERT technique, geochemical analyses show that higher values begin to decrease at shallower layers (2 m in depth) in relation to those for deeper-depth pig slurry ponds. Thus, the latter type of pig slurry ponds could pose a contamination risk to shallow aquifers of the study area (e.g., Quaternary "Campo de Cartagena" aquifer).

Additionally, statistical analysis determines significant correlations between lower resistivity values from internal ERT profiles and the geochemical parameters. This proves that electrical resistivity values are consistent and complementary to geochemical values (pH, EC, salts (Cl, SO_4^{2-}, Na^+), and nitrate ($N-NO^{3-}$) content).

Therefore, the data of this study highlight the potential of the electrical resistivity tomography (ERT) method, in conjunction with boreholes and physicochemical analysis, to identify affected subsurface regions by slurry infiltration. This invaluable data will enable farmers what following stages to undertake in terms of environmental protection.

Author Contributions: Conceptualization, P.M.-P.; data curation, M.G.; funding acquisition, Á.F.; investigation, X.C.-C.; project administration, Á.F.; software, M.A.M.-S.; validation, M.G.; visualization, M.A.M.-S.; writing—original draft, X.C.-C.; writing—review and editing, P.M.-P. All authors have read and agreed to the published version of the manuscript.

Conflicts of Interest: The authors declare no conflict of interest.

References

1. *El Sector de la Carne de Cerdo en Cifras: Principales Indicadores Económicos*; Subdirección General de Producciones Ganaderas y Cinegéticas and Dirección General de Producciones Mercados Agrarios, Ministerio de Agricultura, Pesca y Alimentación: Madrid, Spain, 2020.
2. Caterina, D.; Orozco, A.F.; Nguyen, F. Long-term ERT monitoring of biogeochemical changes of an aged hydrocarbon contamination. *J. Contam. Hydrol.* **2017**, *201*, 19–29. [CrossRef]
3. Martínez-Pagán, P. Aplicación de Diferentes Técnicas no Destructivas de Prospección Geofísica a Problemas Relacionados con Contaminación Ambiental Producida por Diferentes Actividades Antrópicas en la Región de Murcia. Ph.D. Thesis, Universidad Politécnica de Cartagena, Cartagena, Spain, 2006.
4. Rosales, R.M.; Martinez-Pagan, P.; Faz, A.; Bech, J. Study of subsoil in former petrol stations in SE of Spain: Physicochemical characterization and hydrocarbon contamination assessment. *J. Geochem. Explor.* **2014**, *147*, 306–320. [CrossRef]
5. Acosta, J.A.; Martínez-Pagán, P.; Martínez-Martínez, S.; Faz, A.; Zornoza, R.; Carmona, D.M. Assessment of environmental risk of reclaimed mining ponds using geophysics and geochemical techniques. *J. Geochem. Explor.* **2014**, *147*, 80–90. [CrossRef]
6. Aracil Ávila, E.; Maruri Brouard, U.; Vallés Iriso, J.; Martínez Pagán, P.; Porres Benito, J.A. Evaluación de problemas medioambientales mediante tomografía eléctrica. *Geofísica* **2003**, *122*, 34–39.
7. Allred, B.; Daniels, J.J.; Ehsani, M.R. *Handbook of Agricultural Geophysics*; CRC Press: Boca Raton, FL, USA, 2008; pp. 211–233.
8. Samouëlian, A.; Cousin, I.; Tabbagh, A.; Bruand, A.; Richard, G. Electrical resistivity survey in soil science: A review. *Soil Tillage Res.* **2005**, *83*, 173–193. [CrossRef]
9. Chambers, J.E.; Kuras, O.; Meldrum, P.I.; Ogilvy, R.D.; Hollands, J. Electrical resistivity tomography applied to geologic, hydrogeologic, and engineering investigations at a former waste-disposal site. *Geophysics* **2006**, *71*, B231–B239. [CrossRef]
10. Koda, E.; Tkaczyk, A.; Lech, M.; Osiński, P. Application of electrical resistivity data sets for the evaluation of the pollution concentration level within landfill subsoil. *Appl. Sci.* **2017**, *7*, 262. [CrossRef]
11. Yan, Z.; Song, X.; Wu, Y.; Gao, C.; Wang, Y.; Yang, Y. Fingerprinting Organochlorine Groundwater Plumes Based on Non-Invasive ERT Technology at a Chemical Plant. *Appl. Sci.* **2022**, *12*, 2816. [CrossRef]
12. Liao, Q.; Deng, Y.; Shi, X.; Sun, Y.; Duan, W.; Wu, J. Delineation of contaminant plume for an inorganic contaminated site using electrical resistivity tomography: Comparison with direct-push technique. *Environ. Monit. Assess.* **2018**, *190*, 187. [CrossRef]

13. Sainato, C.M.; Losinno, B.N.; Malleville, H.J. Assessment of contamination by intensive cattle activity through electrical resistivity tomography. *J. Appl. Geophys.* **2012**, *76*, 82–91. [CrossRef]

14. Sendrós, A.; Urruela, A.; Himi, M.; Alonso, C.; Lovera, R.; Tapias, J.C.; Casas, A. Characterization of a shallow coastal aquifer in the framework of a subsurface storage and soil aquifer treatment project using electrical resistivity tomography (Port de la Selva, Spain). *Appl. Sci.* **2021**, *11*, 2448. [CrossRef]

15. Netto, L.G.; Barbosa, A.M.; Galli, V.L.; Pereira, J.P.S.; Gandolfo, O.C.B.; Birelli, C.A. Application of invasive and non-invasive methods of geo-environmental investigation for determination of the contamination behavior by organic compounds. *J. Appl. Geophys.* **2020**, *178*, 104049. [CrossRef]

16. Simyrdanis, K.; Papadopoulos, N.; Soupios, P.; Kirkou, S.; Tsourlos, P. Characterization and monitoring of subsurface contamination from Olive Oil Mills' waste waters using Electrical Resistivity Tomography. *Sci. Total Environ.* **2018**, *637*, 991–1003. [CrossRef]

17. Sainato, C.M.; Losinno, B.N.; Malleville, H.J. Electrical resistivity tomography applied to detect contamination on a dairy farm in the Pampean region, Argentina. *Near Surf. Geophys.* **2010**, *8*, 163–171. [CrossRef]

18. Lemeillet, F.; Sainato, C.; Malleville, H.; Carbó, L.; Herrero, A. Electrical conductivity of a soil treated with effluent from livestock. *Geoacta* **2016**, *41*, 57–73.

19. Martínez-Pagán, P.; Faz, A.; Aracil, E. The use of 2D electrical tomography to assess pollution in slurry ponds of the Murcia region, SE Spain. *Near Surf. Geophys.* **2009**, *7*, 49–61. [CrossRef]

20. Sánchez, D.E. Riesgo de heladas por inversión térmica en la huerta de Murcia: Incidencia en la actividad agraria. *Investig. Geográficas (Esp)* **2015**, *64*, 73–86. [CrossRef]

21. Marín Lechado, C.; Roldán García, F.J.; Pineda Velasco, A.; Martínez Zubieta, P.; Rodero Pérez, J.; Diaz Pinto, G. Mapa Geológico continuo de España 1:50,000 Zonas internas de las cordilleras béticas (Zona-2210) in GEODE. In *Mapa Geológico Digital Continuo de España [En Línea]*; Instituto Geológico y MInero de España: Madrid, Spain, 2008.

22. Confederación Hidrográfica del Segura. *Plan Hidrológico de la Demarcación del Segura 2015/21*; Caracterización de las Masas de Agua de la DHS: Madrid, Spain, 2015.

23. Estrella, T.R. Funcionamiento hidrogeológico del campo de Cartagena (Murcia y Alicante). *Hidrogeología* **1995**, *11*, 21–38.

24. Lobera, J.B.; Martínez, P.; Ferrández, F.; Martín, J. *Reutilización Agronómica de los Purines de Cerdo*; Serie técnica y de estudios; Consejería de Medio Ambiente, Agricultura y Agua: Murcia, Spain, 1998.

25. Binley, A.; Slater, L. Resistivity and Induced Polarization. In *Resistivity and Induced Polarization*; Cambridge University Press: Cambridge, UK, 2020; p. 426.

26. Martínez-Segura, M.A.; Vásconez-Maza, M.D.; García-Nieto, M.C. Volumetric characterisation of waste deposits generated during the production of fertiliser derived from phosphoric rock by using LiDAR and electrical resistivity tomography. *Sci. Total Environ.* **2020**, *716*, 137076. [CrossRef]

27. Martín-Crespo, T.; Gómez-Ortiz, D.; Martínez-Pagán, P.; De Ignacio-San José, C.; Martín-Velázquez, S.; Lillo, J.; Faz, A. Geoenvironmental characterization of riverbeds affected by mine tailings in the Mazarrón district (Spain). *J. Geochem. Explor.* **2012**, *119*, 6–16. [CrossRef]

28. Cano, Á.F.; Martínez-Pagán, P.; Ávila, E.A.; Brouard, U.M. Aplicación de la tomografía eléctrica al estudio de los depósitos de estériles mineros "El Lirio" y "Brunita" (Murcia). In *Los Residuos Minero-Metalúrgicos en el Medio Ambiente*; Instituto Geológico y Minero de España (IGME): Madrid, Spain, 2006; p. 89.

29. Martínez-Pagán, P.; Gómez-Ortiz, D.; Martín-Crespo, T.; Martín-Velázquez, S.; Martínez-Segura, M. Electrical resistivity imaging applied to tailings ponds: An overview. *Mine Water Environ.* **2021**, *40*, 285–297. [CrossRef]

30. Constable, S.C.; Parker, R.L.; Constable, C.G. Occam's inversion: A practical algorithm for generating smooth models from electromagnetic sounding data. *Geophysics* **1987**, *52*, 289–300. [CrossRef]

31. DeGroot-Hedlin, C.; Constable, S. Occam's inversion to generate smooth, two-dimensional models from magnetotelluric data. *Geophysics* **1990**, *55*, 1613–1624. [CrossRef]

32. *Instruction Manual for EarthImager 3D Version 1.5.3 Resistivity Inversion Software*; Advanced Geosciences Inc.: Austin, TX, USA, 2008; p. 100.

33. Yang, X.; Lagmanson, M.; Yang, X.; Lagmanson, M. *Comparison of 2D and 3D Electrical Resistivity Imaging Methods. En Symposium on the Application of Geophysics to Engineering and Environmental Problems 2006*; Society of Exploration Geophysicists: Houston, TX, USA, 2006; pp. 585–594.

34. Cobertera, E. *Edafología Aplicada*, 1st ed.; Ediciones Cátedra, S.A.: Madrid, Spain, 1993; p. 326.

35. Andrades, M. *Prácticas de Edafología y Climatología*; Universidad de la Rioja: Logroño, Spain, 1996; pp. 14–16. Available online: https://dialnet.unirioja.es/descarga/libro/194611.pdf (accessed on 18 September 2021).

36. Martínez-Pagán, P.; Cano, Á.F.; Ramos da Silva, G.R.; Olivares, A.B. 2-D electrical resistivity imaging to assess slurry pond subsoil pollution in the southeastern region of Murcia, Spain. *J. Environ. Eng. Geophys.* **2010**, *15*, 29–47. [CrossRef]

37. Straczynska, S. The influence of fertilizing with manure on the soil acidity. *Zesz. Probl. Postępów Nauk. Rol.* **1994**, *413*, 283–285.

38. Chang, C.; Sommerfeldt, T.G.; Entz, T. Rates of soil chemical changes with eleven annual applications of cattle feedlot manure. *Can. J. Soil Sci.* **1990**, *70*, 673–681. [CrossRef]

39. Pozdnyakov, A.I.; Pozdnyakova, L.A.; Karpachevskii, L.O. Relationship between water tension and electrical resistivity in soils. *Eurasian Soil Sci.* **2006**, *39*, S78–S83. [CrossRef]

40. Peralta, N.R.; Cicore, P.L.; Marino, M.A.; da Silva, J.R.M.; Costa, J.L. Use of geophysical survey as a predictor of the edaphic properties variability in soils used for livestock production. *Span. J. Agric. Res.* **2015**, *13*, e1103. [CrossRef]

41. Carrasco, M.; Cecilia, L. Utilización Agronómica de Purines de Cerdo en Brócoli y Sandía en Condiciones Mediterráneas Semiáridas: Influencia en el Sistema Suelo-Planta. Ph.D. Thesis, Universidad Politécnica de Cartagena, Cartagena, Spain, 2005.

42. Carnol, M.; Ineson, P.; Anderson, J.M.; Beese, F.; Berg, M.P.; Bolger, T.; Verhoef, H.A. The effects of ammonium sulphate deposition and root sinks on soil solution chemistry in coniferous forest soils. *Biogeochemistry* **1997**, *38*, 255–280. [CrossRef]

43. Bernal, M.P.; Roig, A.; Madrid, R.; Navarro, A.F. Salinity risks on calcareous soils following pig slurry applications. *Soil Use Manag.* **1992**, *8*, 125–129. [CrossRef]

44. Heiniger, R.W.; McBride, R.G.; Clay, D.E. Using soil electrical conductivity to improve nutrient management. *Agron. J.* **2003**, *95*, 508–519. [CrossRef]

45. Mazaheri, M.R.; Mahmoodabadi, M. Study on infiltration rate based on primary particle size distribution data in arid and semiarid region soils. *Arab. J. Geosci.* **2012**, *5*, 1039–1046. [CrossRef]

46. Oster, J.D.; Shainberg, I. Soil responses to sodicity and salinity: Challenges and opportunities. *Soil Res.* **2001**, *39*, 1219–1224. [CrossRef]

47. Bronick, C.J.; Lal, R. Soil structure and management: A review. *Geoderma* **2005**, *124*, 3–22. [CrossRef]

48. Garcia, G.N. *Química Agrícola: El Suelo y los Elementos Químicos: El Suelo y los Elementos Químicos Esenciales Para la Vida Vegetal*, 2nd ed.; Mundi-Prensa Libros: Madrid, Spain, 2003.

49. Mantovi, P.; Fumagalli, L.; Beretta, G.P.; Guermandi, M. Nitrate leaching through the unsaturated zone following pig slurry applications. *J. Hydrol.* **2006**, *316*, 195–212. [CrossRef]

50. Daudén, A.; Quılez, D. Pig slurry versus mineral fertilization on corn yield and nitrate leaching in a Mediterranean irrigated environment. *Eur. J. Agron.* **2004**, *21*, 7–19. [CrossRef]

51. Piñeiro, C.; Montalvo, G. *La Directiva IPPC Para el Control Integrado de las Emisiones Contaminantes en Ganadería Intensiva de Porcino*; XXI Curso de Especialización FEDNA; En Avances en Nutrición y Alimentación Animal; Fundación Española para el Desarrollo de la Nutrición Animal: Madrid, Spain, 2005; Volume 7, pp. 81–86.

52. Hernandez, R.; Jonathan, O. Determinación de Propiedades de Suelos Agrícolas a Partir de Mediciones Eléctricas Realizadas en Campo y Laboratorio. Master's Thesis, Instituto Potosino de Investigación Científica y Tecnológica, A.C., San Luis Potosi, Mexico, 2019.

53. Dionisi, C.P.; Mignone, R.A.; Rubenacker, A.I.; Pfaffen, V.; Bachmeier, O.; Campitelli, P.A.; Juarez, A.V. Monitoring of physico-chemical parameters of soils after applying pig slurry. Analysis of its application in short and long periods in the province of Córdoba, Argentina. *Microchem. J.* **2020**, *159*, 105545. [CrossRef]

54. Siddiqui, F.I.; Osman, S.B.A.B.S. Simple and multiple regression models for relationship between electrical resistivity and various soil properties for soil characterization. *Environ. Earth Sci.* **2013**, *70*, 259–267. [CrossRef]

55. Michot, D.; Benderitter, Y.; Dorigny, A.; Nicoullaud, B.; King, D.; Tabbagh, A. Spatial and temporal monitoring of soil water content with an irrigated corn crop cover using surface electrical resistivity tomography. *Water Resour. Res.* **2003**, *39*, 1138. [CrossRef]